JOURNAL OF MATERIALS SCIENCE 21 (1986) 1667–1674

Effect of porosity and alumina content on the mechanical properties of compocast aluminium alloy–alumina particulate composite

P. K. GHOSH, S. RAY
Department of Metallurgical Engineering, University of Roorkee, Roorkee 247 667, India

The effects of the size and volume fraction of alumina particles and of the porosity on the tensile strength of Al–4 wt% Mg–alumina compocast particulate composite have been investigated. The contribution of porosity to the reduction in strength of the composite at various levels of alumina content is expressed as a linear function of porosity containing two experimentally determined parameters: σ_0, the ultimate tensile strength at zero porosity level, and α, a weakening factor. For a composite containing a lower level (<7 vol%) of alumina particles, a rapid decrease in the value of σ_0 is observed with an increase in the volume fraction of alumina. The rate of reduction in strength slows down at higher alumina levels in the composite. An increase in particle size is found to reduce the value of σ_0. The value of α is found to decrease with an increase in the volume fraction of alumina in the composite. For a given alumina content the increase in average particle size from 22 to 115 μm is found to push the value of α up a little, followed by a significant decrease with an increase in particle size to 195 μm. The role of porosity in the engineering fracture strain e_f of the composite is found to increase almost linearly with the inverse of porosity above a critical level. For composites with a given level of porosity, e_f is found to increase with an increase in the alumina content of the composite.

1. Introduction

The mechanical properties of compocast particulate composites are very sensitive to the volume fraction of porosity, to the shape, size and distribution of the reinforcing particles, and to their content in the composite. The volume fraction of particles in the composite can be controlled by using suitable process parameters [1] but the porosity cannot be regulated during the process. So far, the mechanical properties of castings have been correlated with the volume fraction of porosity present through a phenomenological model, and verified experimentally for compocast aluminium alloy–alumina composites with a given content of alumina particles [2].

In the present study we have investigated the effects of size and volume fraction of alumina particles with both narrow and wide spectra of sizes on the tensile strength of Al–4 wt % Mg–alumina compocast particulate composite. The contribution of porosity in reducing the strength is estimated at different levels of alumina content, and the projected ultimate tensile strength at zero porosity level is determined. The variation of this strength with alumina content is reported. The role of porosity in the initiation of fracture in these composites is examined.

2. Experimental details

Commercial-purity aluminium of about 500 g was melted in a graphite crucible and the required amount of about 25 g of magnesium lump was added to the melt. The melt was vigorously stirred mechanically at different speeds in the range of 400 to 1500 r.p.m. During stirring the melt was allowed to cool through the solidification range of the alloy until the desired pouring temperature was attained. In different castings, preheated alumina particles with the following size ranges: (+6, −45), (+53, −75), (+106, −125), (+180, −212) μm, and one with a broad spectrum of sizes as mentioned in Table I, were added at the pouring temperature which lies in the semi-solid region of the alloy at a temperature of 900 K. The alumina particles were preheated to 1072 K before adding to the vortex formed on the melt surface by stirring. After the addition of particles the slurry was continuously stirred for 3.75 to 4 min and the temperature was maintained within $\pm$5 K of the pouring temperature. The slurry was then poured into a 25 mm × 30 mm × 300 mm steel mould through the bottom of the crucible by removing the graphite stopper, and the ingot was cooled immediately by spraying water on it. The Al–Mg alloy matrix had the following chemical composition: 4% Mg, 0.98% Fe, 0.3% Si, 0.05% Mn, 0.01% Ti and balance aluminium.

Suitable metallographic samples from both the bottom and top of each casting were prepared using standard metallographic procedures. The specimens were observed under an optical microscope for estimation of the alumina-particle and porosity contents of the composite. The particle–matrix interface was examined under a scanning electron microscope.

0022–2461/86 $03.00 + .12

TABLE I Size distribution of particles in the mixed alumina powder used

Size of alumina particles (μm)	+212	+180, −212	+125, −180	+106, −125	+75, −106	+63, −75	+53, −63	+45, −53	−45
Amount (wt %)	0.31	49.37	13.90	31.56	1.87	1.73	0.33	0.15	0.78

Tensile specimens of the dimesions shown in Fig. 1 were machined from each casting. The volume fraction of alumina particles in each specimen was determined by the point counting method and by using the observed density [1] to calculate the amount of porosity. Tensile tests were carried out on a Hounsfield tensometer at ambient temperature.

Polished and unetched sections perpendicular to the fractured surface of the tensile specimens were observed under a scanning electron microscope. The true strain, ε, at any location in the fractured specimen corresponding to the zone under observation was estimated by measuring the diameter of the specimen at that location as viewed under a scanning electron microscope.

3. Results

A typical distribution of alumina particles in a composite having about 13 vol % particles is shown in Fig. 2. The relation between the standard deviation of the measured volume percentage of particles in a given sample of composite having a specified amount of alumina particles and its porosity content is given in Fig. 3.

The reinforced alumina particles in the composites are found to be well bonded with the matrix, as shown in the scanning electron micrograph in Fig. 4. However, the debonding of alumina particles from the matrix is observed during tensile deformation of the composites. Typical void formation by debonding is depicted in Fig. 5. In this figure it is observed that a large number of voids have been nucleated in the matrix of the composite, at a strain level of about $\varepsilon = 0.325$, during tensile deformation. The path of a crack initiated in a specimen containing ~ 2.75 vol % alumina and fractured under tensile loading is shown in Fig. 6. The formation of a reacted layer of irregular shape around an alumina particle is shown in Fig. 7. The reacted layer is possibly $MgAl_2O_4$, which has been found to form under similar circumstances [3].

The effect of porosity content on the behaviour of the engineering stress–strain curve of a composite having ~ 1.92 vol % alumina is shown in Fig. 8.

The ultimate tensile strength, σ_p, at different volume percentages of porosity, P, was obtained for samples containing a known amount of alumina particles. Our earlier investigation [2] amply justifies the assumption of linear behaviour of σ_p with P in this class of materials, in spite of the scatter observed. The scatter is attributed to the limitations of a one-parameter model in describing the shape and size distribution of the pores affecting the ultimate tensile strength. However, it should be noted that the correlation coefficient was found to be better than 0.85 in the earlier investigations. A linear least-squares fit of the observed σ_p with P was carried out following the model equation proposed earlier [2]:

$$\sigma_p/\sigma_0 = 1 - \alpha P \quad (1)$$

where σ_0 is the ultimate tensile strength at zero porosity for each alumina content and α is the weakening factor of the pores. The variation of α with alumina content is depicted in Fig. 9. It is observed that the value of α decreases with an increase in the volume fraction of alumina in the composite.

Fig. 10 shows the relationship between the particle content and the tensile strength at zero porosity, σ_0, for different composites containing alumina particles having a wide range of sizes as given in Table I. The value of σ_0 is found to decrease rapidly with an increase of the volume fraction of alumina, up to around 7% in the composite. A further increase in the volume fraction of alumina content up to around 18% is found to reduce the tensile strength of the composite very slowly.

The value of σ_0 is found to decrease with an increase in the average particle size from 22 up to 195 μm for composites containing a fixed amount (~ 8.62 vol %) of alumina, as shown in Fig. 11. The magnitude of the corresponding weakening factor α is found to increase a little with an increase in the average particle size from 22 to 115 μm, followed by a significant decrease with further increase in particle size to 195 μm as shown in Fig. 12.

In Fig. 13 the engineering fracture strain, e_f, is plotted against the reciprocal of the percentage of porosity content in composites with a given amount of volume fraction of alumina particles having a broad

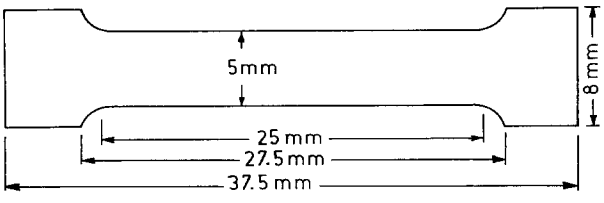

Figure 1 Dimensions of the tensile specimen.

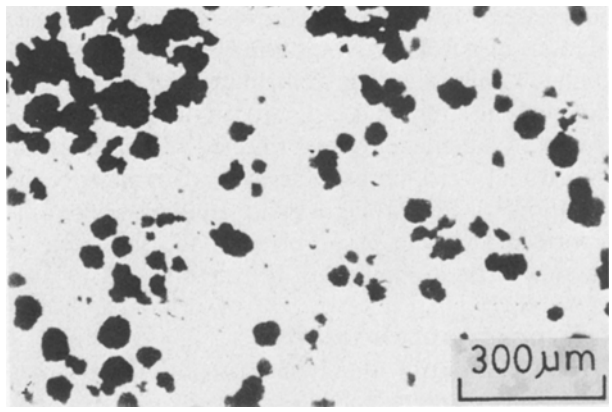

Figure 2 Typical distribution of alumina particles in the composite.

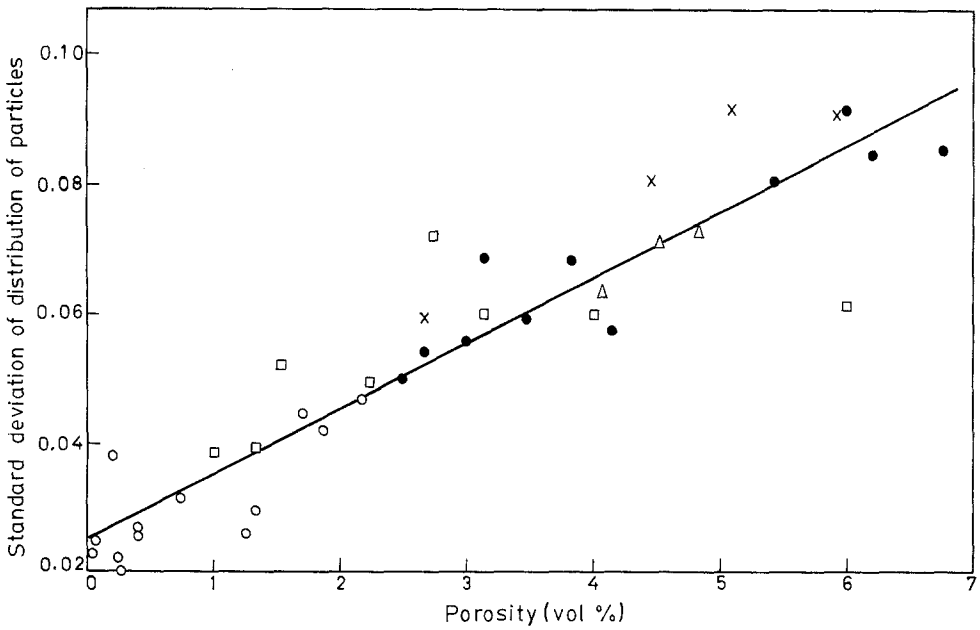

Figure 3 Effect of standard deviation of distribution of particles on the porosity content of the composite. Approximate volume percentage of alumina: (○) 1.6 ± 0.2, (□) 5.6 ± 0.3, (●) 9.5 ± 0.45, (×) 11.0 ± 0.5, (△) 14.6 ± 0.4.

spectrum of sizes (as given in Table I). The e_f of the composites increases linearly with a decrease of porosity content, but only up to a certain limit. The nature of the curves can approximately be described by the equation

$$e_f = c + m/P \quad (2)$$

where c and m are constants. The slope of the line, m, increases with an increase in the alumina content of the composite as shown in Fig. 14. However, the value of c decreases linearly with an increase in the alumina content as shown in Fig. 15. The linear nature of the e_f against $1/P$ curve is violated when the porosity is reduced below a critical level depending on the alumina content. A further reduction in porosity lowers e_f, as is evident for the composites containing 0.77, and 1.5 and 9.0 vol % alumina.

4. Discussion

The level of porosity in a compocast composite is directly correlated with the inhomogeneity in particle distribution. It has been observed from microscopic investigations that a well-separated particle does not generally have a void at the interface, but a cluster of particles often has voids. During particle addition in the semi-solid melt the stirring employed creates a negative pressure at the centre of the stirrer, and air bubbles are sucked into the melt along with a few particles. The particles may subsequently get transferred from the bubble to the melt and the bubble floats to the top. In the case of certain bubble–particle configurations, particle transfer from the bubble may not be dynamically feasible and clusters of particles are observed in the microstructure along with voids. There may be clusters without voids resulting from sintering together of the particles. However, the increase in porosity with a tendency for clustering shows the former mechanism of cluster formation to be the dominant one. It is evident from Fig. 3 that a higher level of porosity results from an increased tendency for particle clustering. In addition, these clusters with voids are creating inhomogeneous regions of weakness.

The contribution of porosity to the tensile strength of a material has been estimated grossly as a weakening effect caused by the formation of a weakened zone

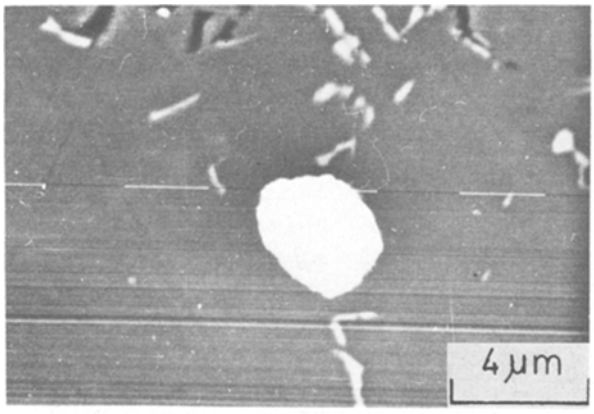

Figure 4 Scanning electron micrograph showing bonding of alumina particle with the matrix.

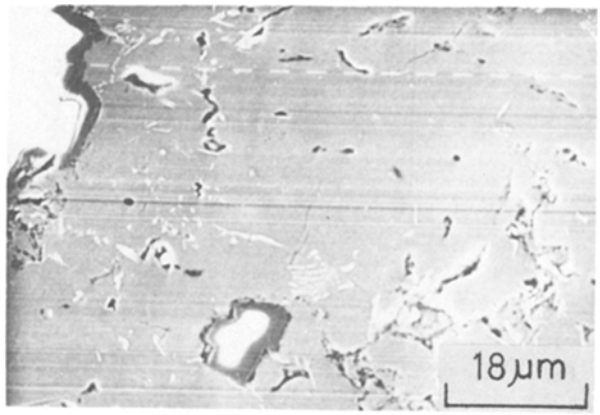

Figure 5 Scanning electron micrograph showing debonding of particle–matrix interface and presence of voids in the matrix.

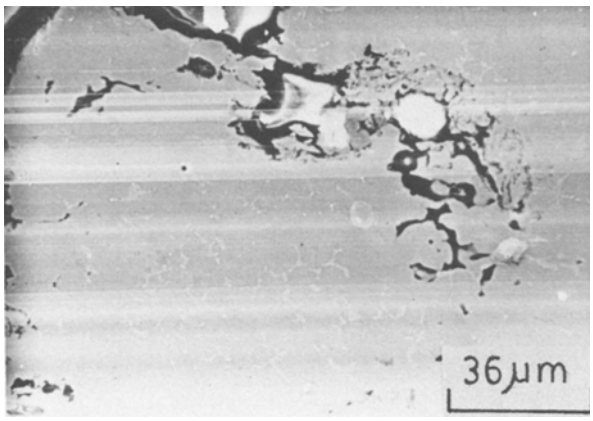

Figure 6 Nature of a crack path in a composite fractured under tensile loading.

around a spherical pore, and is given by Equation 1. The equation is derived by assuming that the pore has no damaging effect on the load-bearing capacity of a material beyond a certain distance $R_p = nr_p$ from the pore, where r_p is the average effective radius of the pore and n is a constant having a value greater than unity which is primarily dependent on the mechanical characteristics of the material. The weakening of the material also depends on the geometry of the pore and on the the pore distribution. The average stress at $r = r_p$ is $k\,\sigma_m$ where k is a constant factor and σ_m is the stress in regions unaffected by the pore. The averaging is performed over the size distribution of the pores and the angles around the axis of loading. The weakening of the material will limit the value of k in the range $0 < k < 1$. The weakening factor α is a function of both the parameters n and k. Equation 1 is capable of estimating the contribution of the pore in the linear regime up to a porosity level P_c given by

$$P_c = 100/n^2 \qquad (3)$$

For a higher porosity level, Equation 1 is not effective because the stress distributions around pores start interfering with each other; this results in an effective pore–pore interaction term when R_p is greater than R, where R is the radius of the average volume of material per pore.

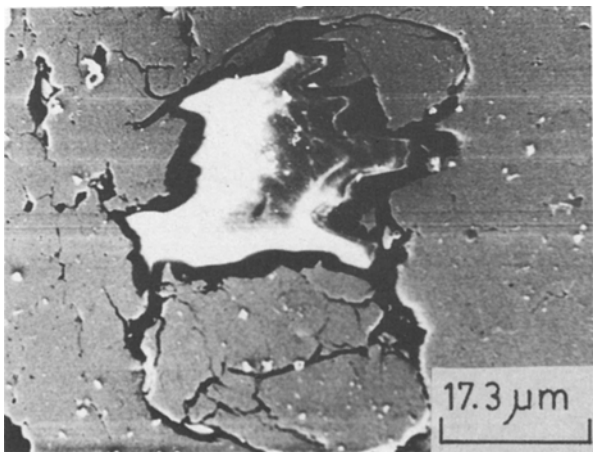

Figure 7 Scanning electron micrograph showing the formation of a reacted layer of irregular shape around an alumina particle.

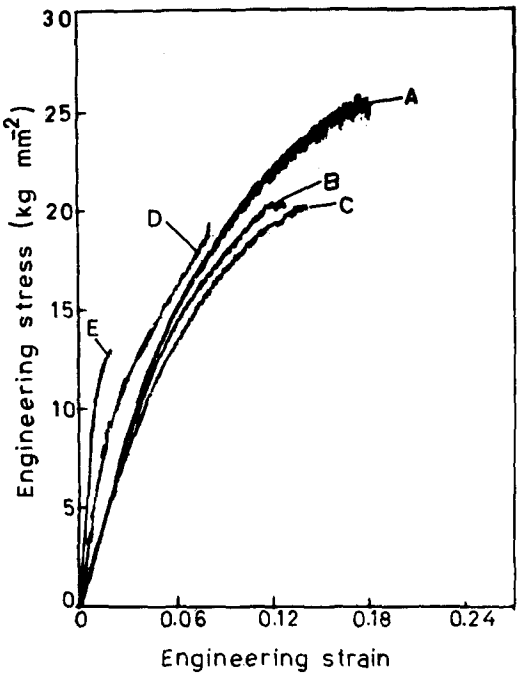

Figure 8 Effect of porosity content on engineering stress–strain curve of a particulate composite. Approximate porosity (vol %): (A) 0.76, (B) 0.82, (C) 0.95, (D) 1.5, (E) 6.0. Content of $Al_2O_3 \sim 1.92$ vol %.

When the porosity is above a critical level depending on the alumina content of the composite, the correlation of the inverse of as-cast porosity with fracture strain shows a linear behaviour with coefficient exceeding 0.9, as shown in Fig. 13. In this range of porosity the failure is caused primarily by the growth and coalescence of pores confined primarily to the regions of particle cluster. The voids nucleated during deformation at the boundary between a well-bonded particle and the matrix are not responsible for the fracture of these composites. Fig. 5 clearly demonstrates extended voids created by the growth and linkage of pre-existing voids at the boundaries of alumina particles and microporosities away from the particles. However, Fig. 6 (showing the microstructure of a transverse section near the fractured surface) demonstrates that void growth and coalescence are confined to the inhomogeneous regions containing particle clusters with voids. The matrix away from this weak zone is relatively free from damage.

The serrated nature of the tensile stress–strain curve as given in Fig. 8 is an indication of continuing void coalescence over the range of strain. From the above discussion it is inferred that although debonding at the alumina–matrix interface might have taken place, the failure is primarily caused by existing voids as evident in Fig. 5. So the present approach to explaining the properties on the basis of a model incorporating the role of pre-existing pores is thus justified. The particles are assumed to exert only a secondary influence by modifying the parameters of the model Equation 1 for ultimate tensile strength.

The experimental observations presented in Fig. 9 show that the weakening factor α in a particulate composite decreases with the volume fraction of reinforcing alumina particles. Since the particles used for this set of experiments have the same broad

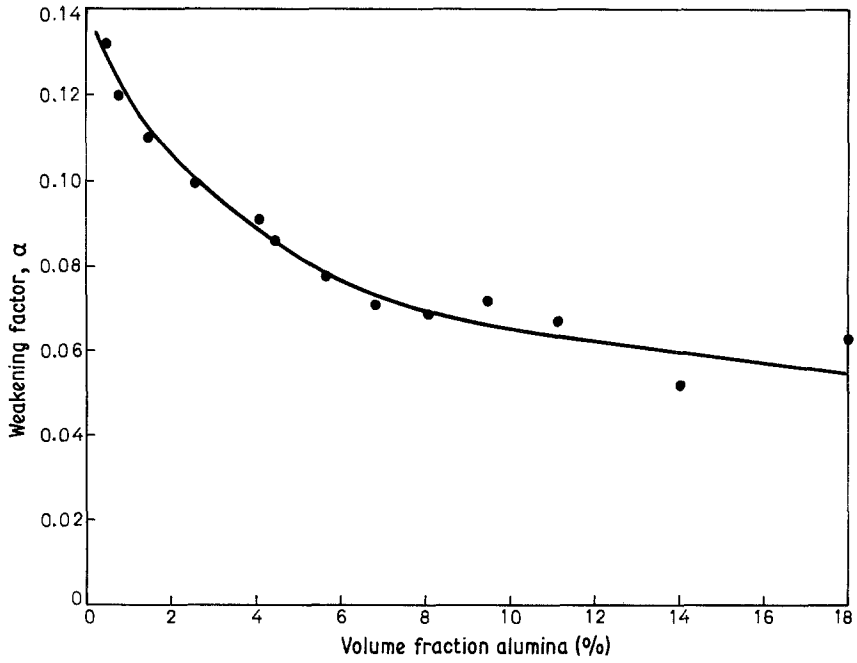

Figure 9 Variation of weakening factor with alumina content of the composite.

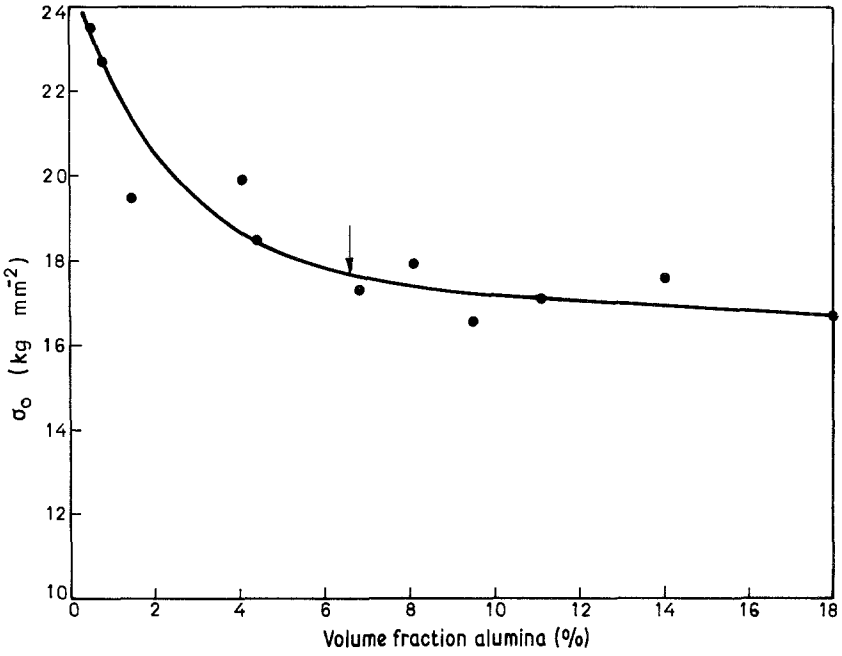

Figure 10 Effect of particle content on tensile strength of the composite at zero porosity. The arrow indicates the strength of Al–4.0 wt % Mg without alumina, extrapolated to zero porosity.

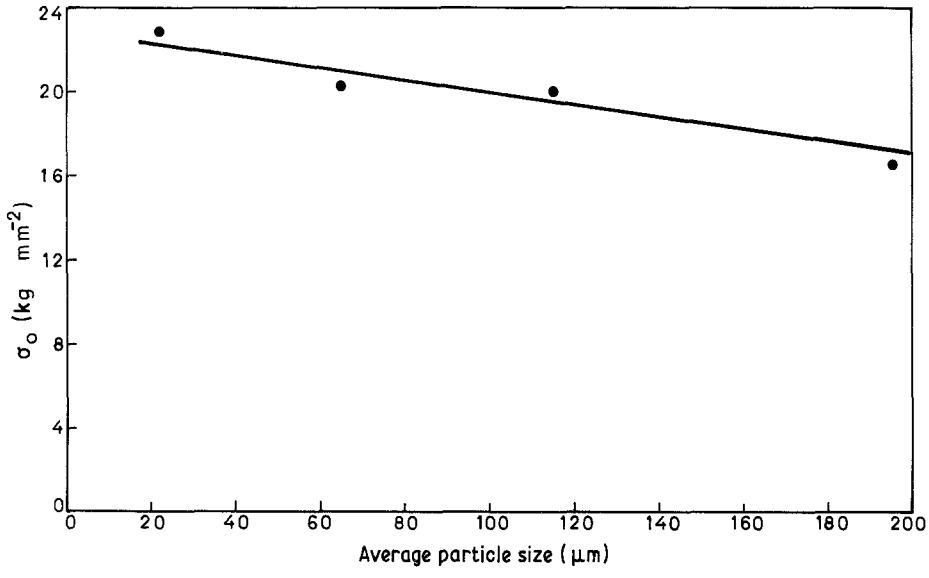

Figure 11 Effect of average particle size on tensile strength of the composite at zero porosity.. Volume fraction of alumina $\sim 8.62 \pm 0.6\%$.

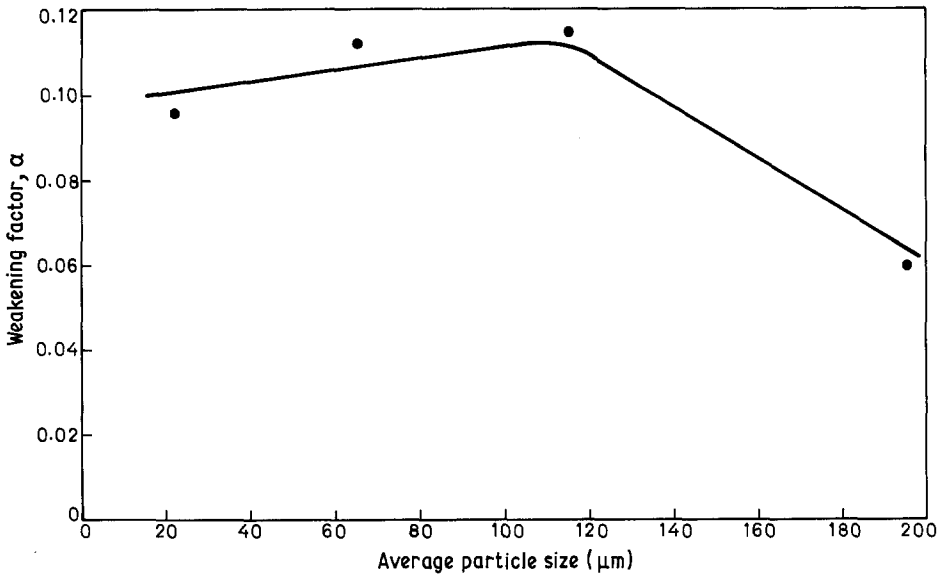

Figure 12 Variation of weakening factor with average particle size in the composite. Volume fraction of alumina ~8.62 ± 0.6%.

spectrum of size distribution, so the increase in volume fraction indicates an increase in the number of particles per unit area of matrix. The spatial recovery of the load-bearing capacity will be affected by the presence of a foreign particle because of the modification in the stress distribution around it. Thus, both n and k may be modified to cause the observed lowering of the weakening factor α. However, this enhancement of α becomes less marked at higher particle content in the composites.

The lowering of tensile strength, σ_0, with an increase of the volume fraction of reinforced particles shown in Fig. 10 is caused by the nucleation of voids at the particle–matrix interface. The void is initiated in the particle–matrix interface at early stages of plastic deformation [4], and reduces the load-bearing capacity of the material at a strain which falls with an increase in alumina content. Moreover the formation of $MgAl_2O_4$ [3] in irregular extended shapes with sharp corners is observed to create particularly susceptible areas for the generation of cracks as shown in Fig. 7. Fragmentation of brittle $MgAl_2O_4$ is commonly observed. However, the observed σ_0 of the composite is superior to the strength of the matrix at zero porosity level up to about 6.5 vol % alumina. Beyond this level of incorporation of alumina the room-temperature strength possibly degenerates.

From a consideration of the growth of voids under stress Brown and Embury [5] have given the criteria for estimating the critical strain, ε_g, at which the necking instability in the material between two growing voids will cause the joining of voids. This strain,

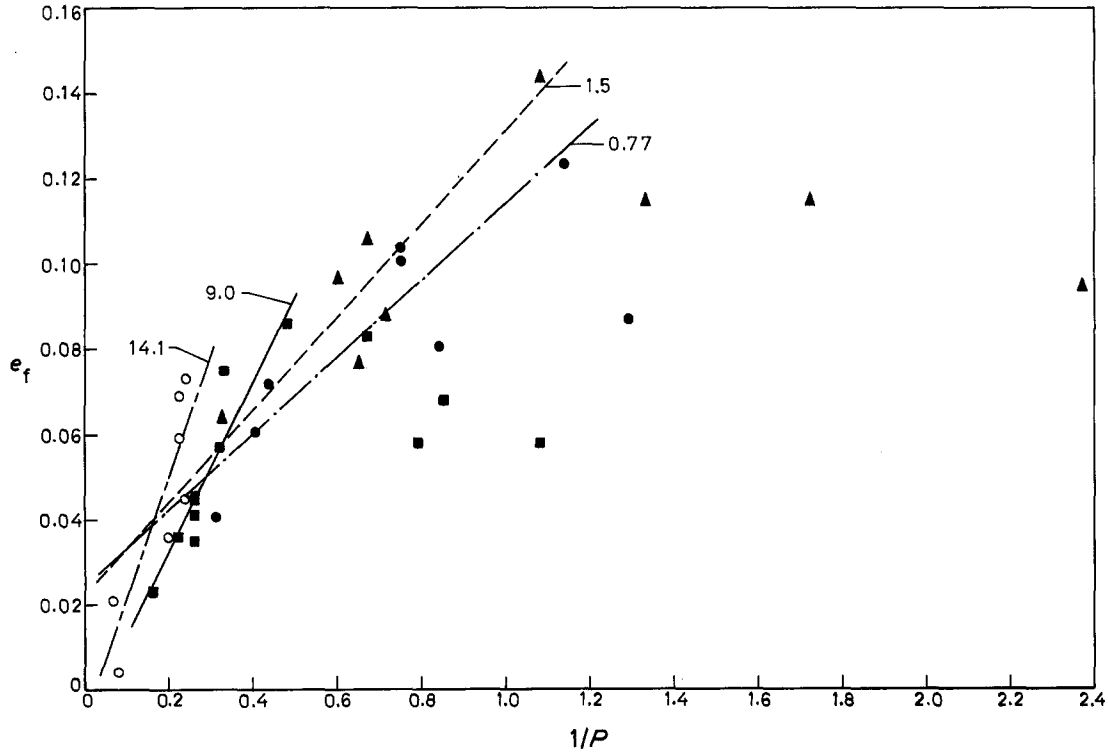

Figure 13 Effect of the inverse of volume percentage of porosity on engineering fracture strain for composites containing various volume fractions of alumina. Approximate volume percentage of alumina: (●) 0.77 ± 0.06, (▲) 1.50 ± 0.12, (■) 9.00 ± 0.42, (○) 14.10 ± 0.47.

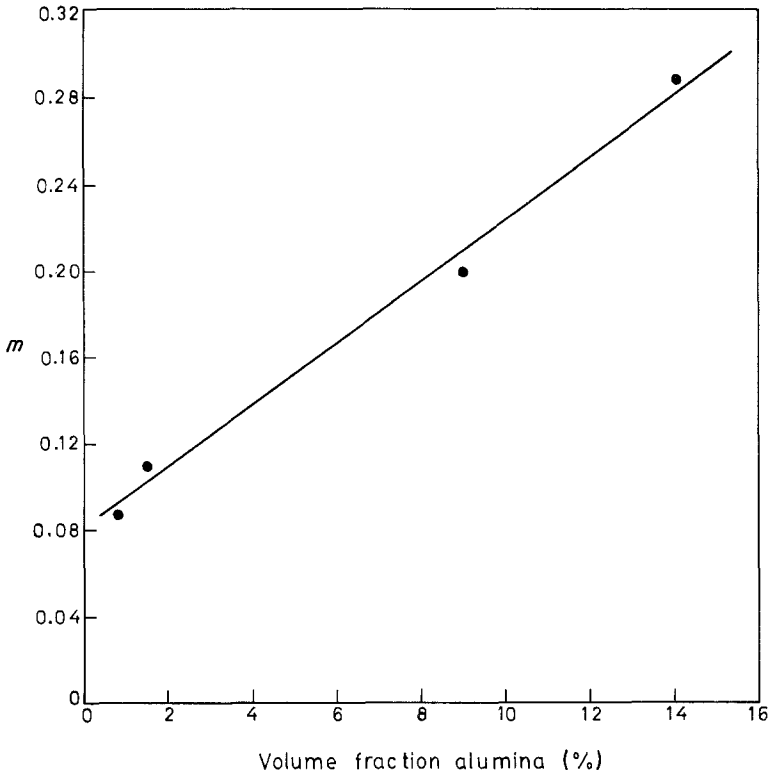

Figure 14 Effect of alumina content of the composite on the slope m of the equation $e_f = c + m/P$.

together with the nucleating strain ε_n for the voids, will constitute the fracture strain. They proposed

$$1 + \varepsilon_g = \frac{1}{2}\left[\left(\frac{2\pi}{3f}\right)^{1/2} - \left(\frac{8}{3}\right)^{1/2}\right] \quad (4)$$

where f is the volume fraction of particles, keeping the size of the particles constant. So it is expected that ε_g and the corresponding stress will decrease non-linearly with the volume fraction of particles, as observed in the behaviour of σ_0 shown in Fig. 10. However, it must be remembered that in the cast materials with porosity this picture will be modified by the growth of already existing porosity, for which the nucleating strain is zero.

For the same volume fraction of particles, if the particle size is increased (i.e. interparticle spacing is reduced) one expects a delayed onset of the necking instability. However, the results shown in Fig. 11 show a contrary trend which is in agreement with earlier investigations [4, 6] and can be explained in terms of a lower ε_n for the nucleation of voids around particles having a larger size. This effect, along with a larger initial size of the void, offsets the advantage gained by a larger interparticle spacing.

A small initial enhancement of the weakening factor α with an increase in the average particle size upto $\sim 115\,\mu$m, as shown in Fig. 12, may be due to a decrease in the number of particles in the weakened zone. But the subsequent decrease in the value of α with an increase of particle size beyond $\sim 115\,\mu$m indicates an important role of the particle in modifying the stress distribution of the weakened zone, thus resulting in a higher degree of recovery of the lost strength.

The true fracture strain has been correlated with the inverse of the volume fraction of voids by several

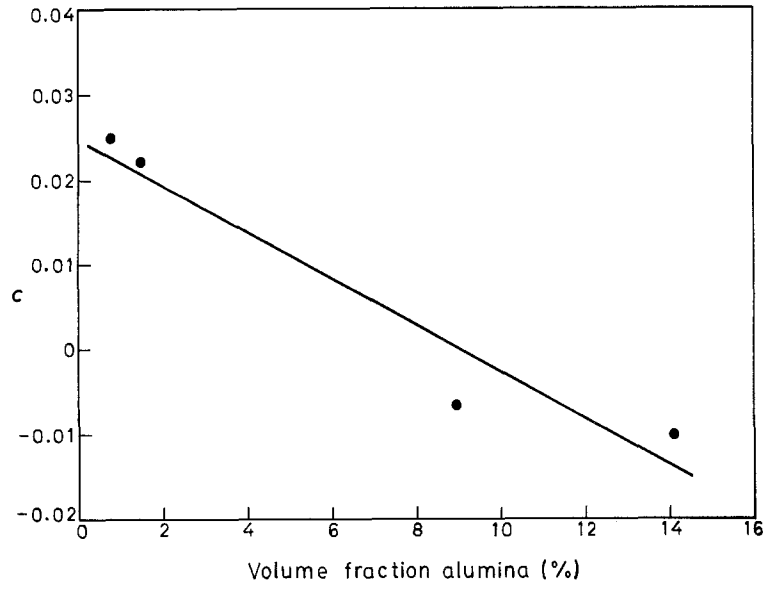

Figure 15 Effect of alumina content of the composite on the value of c of the equation $e = c + m/P$.

authors [7–9]. The engineering fracture strain observed in the present investigation has been plotted against the inverse of porosity content (as shown in Fig. 13) to identify the role of porosity in determining the fracure behaviour. Above a particular value of porosity the fracture strain increases almost linearly with the inverse of porosity. In this regime of porosity content, the variation of fracture strain with porosity has been represented by the Equation 2 and the particle content is found to influence both m and c as given in Figs. 14 and 15, respectively. These figures indicate that the engineering fracture strain is higher for composites with a higher alumina content, resulting in higher values of m. The factor c, which makes a smaller contribution to e_f compared with m/P and is distributed around zero, may have appeared because of a random error introduced by the limitations of our measurements.

References

1. P. K. GHOSH, S. RAY and P. K. ROHATGI, *Trans. Jpn Inst. Metals* **25** (6) (1984) 440.
2. P. K. GHOSH, P. R. PRASAD and S. RAY, *Z. Metallkde* **75** (1984) 934.
3. B. F. QUIGLEY, G. J. ABBASCHIAN, R. WUNDERLIN and R. WUNDERLIN and R. MEHRABIAN, *Met. Trans.* **13A** (1) (1982) 93.
4. K. TANAKA, T. MORI and T. NAKAMURA, *Phil. Mag.* **21** (1970) 267.
5. L. M. BROWN and J. D. EMBURY, in Proceedings of 3rd International Conference on the Strength of Metals and Alloys, Cambridge, England, August 1973, "The Microstructure and Design of Alloys" (The Institute of Metals and Iron and Steel Institute, London, 1973) Vol. 1, p. 164.
6. V. M. SERGEENKOVA, V. P. DUBININ and V. V. OSASYUK, *Poroshkovaya Met.* **6** (1969) 81.
7. T. GLADMAN, B. HOLMES and I. D. McIVOR, "Effect of Second-Phase Particles on the Mechanical Properties of Steel" (Institute of Metals, London, 1971) p. 68.
8. J. F. KNOTT, "Fundamentals of Fracture Mechanics" (Butterworths, London, 1973). Ch. 8.
9. B. I. EDELSON and W. M. BALDWIN, *Trans. Amer. Soc. Metals* **55** (1962) 230.

Received 10 September 1984
and accepted 4 July 1985